MISO visible light communication system utilizing hybrid post-equalizer aided pre-convergence of STBC decoding

Liang Qiao (乔 梁), Xingyu Lu (卢星宇), Shangyu Liang (梁尚雨), Jiao Zhang (张 教), and Nan Chi (迟 楠)*

Shanghai Institute for Advanced Communication and Data Science, Key Laboratory for Information Science of Electromagnetic Waves (MoE), Fudan University, Shanghai 200433, China

**Corresponding author: nanchi@fudan.edu.cn*

Received February 11, 2018; accepted April 19, 2018; posted online May 28, 2018

In this Letter, we propose a modified hybrid linear and nonlinear post-equalizer to aid pre-convergence of space–time block coding (STBC) decoding in the formulated multiple-input-single-output (MISO) visible light communication (VLC) model. Meanwhile, we present a channel estimation algorithm, as the existing method is suboptimal. Experiments demonstrate that a data rate of 1 Gbit/s is easily achieved in 1.3 m indoor free space transmission with the bit error rate (BER) limited to 3.8×10^{-3}. Correspondingly, the Q factor can be improved to 3.13 dB compared to the pure linear equalizer case.

OCIS codes: 060.4080, 060.4230.
doi: 10.3788/COL201816.060604.

Over the past few years, visible light communication (VLC) has received significant attention to moving parts of high-speed indoor data transmission. Unlike radio frequency (RF) wireless communication, VLC utilizes the already installed light emitting diode (LED) as data transmitters (Tx)[1–5] that can be applied in environments where RF is not necessarily allowed, such as airplanes and military facilities. Except, VLC has also been standardized for wireless personal area networks (WPANs) in Institute of Electrical and Electronics Engineers (IEEE) standard 802.15.7, and it aims to open the road for commercialization in both industry and academia[6].

However, limited modulation bandwidth is one of the obstacles to improve the transmission rate for the VLC system[7–10]. Meanwhile, VLC is generally line-of-sight (LOS) and cannot propagate through walls. One straightforward method is that several LED lamps are jointly deployed, which also meet the lighting demand[11]. The most common method to improve the quality of the signal is employing multiple-input-single-output (MISO) or multiple-input-multiple-output (MIMO) technology combined with LED arrays[12]. The authors in Ref. [13] proved the feasibility of beam-forming in the MISO-VLC system. Besides, one challenge is that the correlation between the spatial channels in a multi-dimensional transmission system employing a non-imaging receiver is high; the size of receiver arrays has to be several distances to ensure that the channel matrix is full-rank. Therefore, a diversity algorithm named space–time block coding (STBC) is demonstrated in Refs. [14,15] and 49-quadrature amplitude modulation (QAM) is generated with the modulation of 16-QAM in both Txs. The reason is that the transmitted symbols must be non-negative and real-valued, as information is communicated by modulating the intensity of the light emitted by LEDs and direct detection (DD) via photodiodes (PDs) for recovery.

In the multi-dimensional system, linear damage will lead to the intersymbol interference (ISI)[16,17]. Some linear post-equalization algorithms, such as recursive least square (RLS) and least mean square (LMS) act as the savior to eliminate ISI. However, these two equalization algorithms require a certain length of training sequence (TS). Instead, some researchers proposed blind equalization to adaptively revise distorted signals, such as multi-modulus algorithm (MMA), cascaded-MMA (CMMA) and the modified CMMA (MCMMA)[18].

The LED nonlinearity by electrical amplifiers (EAs) and optoelectronic devices also distorts signals and deteriorates the system performance. Therefore, the compensation for nonlinearity has gradually become one of the significant challenges in the VLC system. Pre-distortion and post-distortion techniques generally go hand-in-hand, and both are valid solutions to mitigate the VLC channel artifacts[19,20]. However, the above two literatures are only validated by simulation results and lack of experimental demonstration. As a promising solution, the Volterra-series-based equalizer plays a role of significance to mitigate the LED nonlinearity[21]. In our previous work, a blind post-equalization scheme called cascaded Volterra modified MMA was employed and demonstrated to compensate for linearity and mitigate the LED nonlinearity in a carrierless amplitude phase (CAP) modulation-based VLC system[22]. The authors in Ref. [23] employed MCMMA to equalize received signals in the MISO-STBC system. The experiments demonstrate that it also aids pre-convergence of STBC decoding at the receiver. However, the compensation for nonlinearity is never considered.

 © 2018 Chinese Optics Letters

In this Letter, we present a modified hybrid linear and nonlinear post-equalizer to mitigate the nonlinear distortion based on our previous work[23]. Extensive lab experiments demonstrate that the hybrid post-equalizer is also an excellent complementary technology for STBC decoding. Meanwhile, we propose an optimization algorithm for channel estimation, as the existing method in Ref. [23] is suboptimal. With these improved algorithms, a data rate of 1 Gbit/s is easily achieved in 1.3 m of indoor free space transmission with the bit error rate (BER) below the 7% forward error correction (FEC) limited to 3.8×10^{-3}. The Q factor can be improved to 3.13 dB compared to the pure linear equalizer case. To the best of our knowledge, this is the first time that the Volterra-based nonlinear equalizer is demonstrated in the high-speed single-carrier VLC-MISO system.

First, we formulate an MISO-STBC model with the modulation of QAM to investigate the proposed hybrid post-equalizer performance. An indoor VLC-MISO system has the number of LEDs and PDs of N_T and 1, respectively. The input data X is modulated by the intensity of light and superimposed on the direct current (DC).

Before the in-phase and quadrature (I–Q) modulation, Alamouti's STBC schemes encode the data as follows:

$$\begin{bmatrix} x_1 & -x_2^* \\ x_2 & x_1^* \end{bmatrix},$$

where x_1 and x_2 are complex signals to be transmitted, and * denotes the conjugate operation.

The VLC-MISO model can be expressed by

$$Y(t) = H(t) \cdot \begin{bmatrix} x_1(t) & -x_2^*(t) \\ x_2(t) & x_1^*(t) \end{bmatrix} + N(t), \tag{1}$$

wherein the received signal vector is expressed by $Y = [y_1, y_2, \ldots, y_N]^T$. $H(t)$ and $N(t)$ denote the channel matrix and thermal noise, respectively.

In this model, two QAM symbols encoded by STBC are mapped into sixteen constellations. As the symbols must be non-negative and real-valued, the received signals of 49-QAM are generated, as it employed instant messaging (IM) via LEDs for transmission and DD via PDs for recovery. However, the forty-nine constellations are rolled into a mass by the VLC-LOS propagation loss, and then, the signals cannot be recovered by STBC decoding.

The MMA is one of the classic and simple blind equalizations to avoid extra phase rotation[24]. In parallel, the nonlinearity is more obvious as to higher modulation orders appearing, which is also a Gordian knot in the multi-dimensional VLC system with few investigated before. The Volterra series theory has been verified as an alternative way to compensate the nonlinearity. In this article, a modified hybrid Volterra-MCMMA based on Ref. [22] is proposed.

Theoretically, if more terms are used to estimate the original symbols, the results will be more accurate. In fact, the complexity of the Volterra series is too high. As a tradeoff between equalization performance and computational complexity, only the second order terms are taken into consideration[25]:

$$y(m) = \sum_{i=0}^{N-1} h_i(m) \cdot x(m-i) + \sum_{i=0}^{N-1} \sum_{k=i}^{N-1} h_{ik}(m) \cdot x(m-i) \cdot x(m-k), \tag{2}$$

where h_i and h_{ik} are the coefficients for each polynomial term with different orders. N is the memory length of the Volterra series.

The hybrid equalizer includes linear equalization and nonlinear equalization:

$$y(m) = \sum_{i=0}^{N-1} w_i(m) \cdot x(m-i) + \sum_{i=0}^{NI-1} \sum_{k=i}^{NI-1} w_{ik}(m) \cdot x(m-i) \cdot x(m-k). \tag{3}$$

Wherein, the output of $y(m)$ is the linear sum of the two equalizers. N and NI are the tap numbers of the linear and the nonlinear equalizer. w_i and w_{ik} are the weights of the linear and nonlinear equalizers, respectively.

Unlike the method in Ref. [22], the coefficients of the transfer function of I–Q components will be updated individually. Its cost function is expressed as

$$\begin{aligned} \delta_I &= ||||y_I(m)|\text{-}\sigma_1|\text{-}\sigma_2|\text{-}\sigma_3|\text{-}\sigma_4 \delta_Q \\ &= ||||y_Q(m)|\text{-}\sigma_1|\text{-}\sigma_2|\text{-}\sigma_3|\text{-}\sigma_4, \end{aligned} \tag{4}$$

where σ_1, σ_2, σ_3, and σ_4 represent the pre-convergence values of the real and imaginary parts of the 49-QAM signal. M_I and M_Q are sign factors for the I–Q components in MCMMA, respectively. Therefore, the coefficient update equation of the modified hybrid post-equalizer is

$$\gamma(m+1) = \gamma(m) + \mu \cdot (\delta_I \cdot M_I + j \cdot \delta_Q \cdot M_Q) Z^*(m), \tag{5}$$

where * is the Hermitian symbol, and $Z(m) = \{z^2(m), z^2(m-1), \ldots, z^2(m-k)\}$.

At the receiver, the modified hybrid post-equalizer block diagram can be structured, as in Fig. 1. We find that forty-nine constellations are distinct after the proposed hybrid post-equalizer.

In this model, we need the channel matrix to decode received symbols. The recovery signals can be expressed as

$$\begin{aligned} \tilde{X}(t) &= H^{-1}(t) \cdot Y(t) + \tilde{N}(t) \\ &= \begin{bmatrix} h_1(t) & h(t) \\ h_2^*(t) & -h_1^*(t) \end{bmatrix} \cdot Y(t) + \tilde{N}(t). \end{aligned} \tag{6}$$

To access to slightly accurate channel information, we insert a shorter length of TSs in front of STBC symbols.

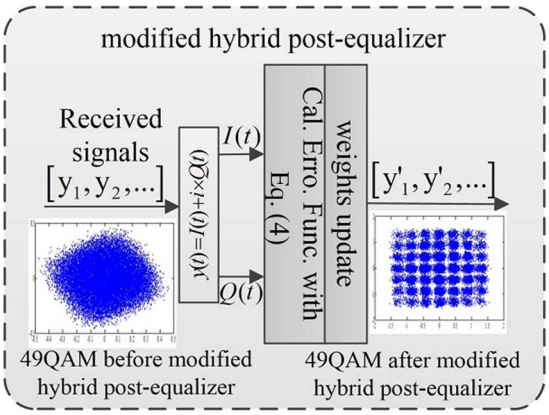

Fig. 1. Schematic of the modified post-equalizer at the receiver.

We get a better channel matrix according to vast calculations offline and the analysis:

$$\begin{bmatrix} h_{s\_n}(t) & h_{s\_n+1}(t) \\ h^*_{s\_n+1}(t) & -h^*_{s\_n}(t) \end{bmatrix} = \begin{bmatrix} c & c \\ c & -c \end{bmatrix}. \tag{7}$$

Wherein, the magnitude of c in $H^{-1}(t)$ is the same. We conclude the reasoning as follows:

- The formulated MISO-STBC model is only demonstrated in the LOS environment;
- The distance between LED1 and the PD is the same as the distance between LED2 and the PD;
- The signal strength from the two LEDs is the same.

In principle, the longer the TSs length, the easier for STBC decoding. Actually, as we concluded recently, the length of the TS had little effect on the c. In this Letter, the length of the TS is thirty symbols in each LED with the method of time division multiplexing (TDM)[26].

Subsequently, we assume

$$H^{-1}(t) = \sum_{n=1}^{N} \begin{bmatrix} h_n(t) & h_{n+1}(t) \\ h^*_{n+1}(t) & -h^*_n(t) \end{bmatrix}. \tag{8}$$

Wherein, n is the index of the transmitted symbol, the magnitude of $h_n(t)$ is the same as $h_{n+1}(t)$, and an error function is defined as

$$\sum_{n=1}^{N} \min\{\|h_n(t)\| - \|h^*_n(t)\|, \|h_{n+1}(t)\| - \|h^*_{n+1}(t)\|\} \le \varepsilon. \tag{9}$$

As analyzed formerly, the loss in the VLC-LOS channel can be assumed to be the same. However, different elements of the matrix experience different losses. The purpose of Eq. (9) is to choose an optimal value that satisfies the condition of minimum path loss. Therefore, we get the optimal channel matrix according to Eq. (9):

$$H^{-1}_{\text{opt}}(t) = \begin{bmatrix} h_{sn}(t) & h_{sn}(t) \\ h^*_{sn}(t) & -h^*_{sn}(t) \end{bmatrix}. \tag{10}$$

Finally, we employ $H^{-1}_{\text{opt}}(t)$ for STBC decoding. Therefore, Eq. (6) can be rewritten as

$$\begin{aligned} \tilde{X}(t) &= H^{-1}(\mathrm{t}) \cdot Y(t) + \tilde{N}(t) \\ &= \begin{bmatrix} h_{sn}(t) & h_{sn}(t) \\ h^*_{sn}(t) & -h^*_{sn}(t) \end{bmatrix} \cdot Y(t) + \tilde{N}(t). \end{aligned} \tag{11}$$

Figure 2 depicts the experimental setup of the formulated MISO-STBC system. Two QAM-STBC signals are modulated and encoded by offline MATLAB with the same parameters set as follows: number of bits of 30000, number of training signals of 30. To compensate channel fading, the impulse response of two filters form a Hilbert pair, and the square root raised-cosine function $g(t)$ is used as the baseband impulse response with the roll-off coefficient $\partial = 0.2$. Subsequently, the transmitted signals are generated using an arbitrary waveform generator (AWG, Tektronix® AWG520). Two electrical QAM-STBC signals are first fed into two pre-equalizers and amplified by EAs, then superimposed onto the LED bias current by the aid of a bias-tee. The transmitted signals

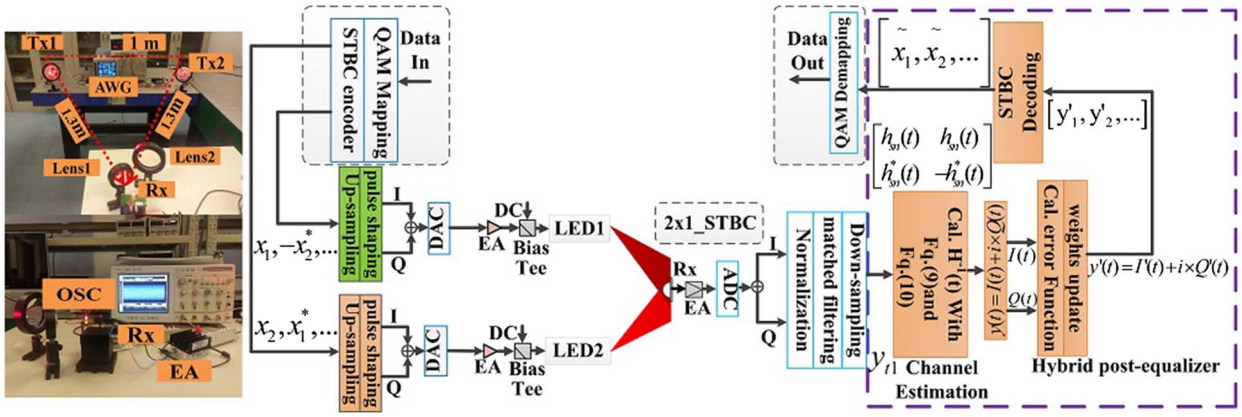

Fig. 2. Block diagram and experimental setup in the MISO-STBC system.

are carried by the red light of red–green–blue (RGB) LEDs. The distance between Tx1 and Tx2 is 1.0 m. After a free space link, the two optical QAM-STBC signals are directly detected by the PD. Two aspheric lenses are in front of the PD, which is to make sure that the light transmits along the 1.3 m perpendicular direction. As the received signal stream is a linear combination of the transmitting signal from Tx1 and Tx2, the MISO system is realized. Finally, the signals are received and down-sampled by an Agilent 54855A digital oscilloscope. The main works of offline MATLAB are as follows: to equalize the received signals with a modified hybrid post-equalizer by Eq. (4), calculate the optimized channel matrix by Eqs. (9) and (10), and decode the signals by Eq. (11).

First, we investigate the BER versus signal strength of different LEDs without the proposed channel estimation algorithm.

As is shown in Fig. 3, 16-QAM is utilized in both LEDs, and the sample rate from the AWG is fixed at 1 GSa/s. The upper two figures depict BER versus the bias voltages (DC voltages) of different LEDs. One is fixed at 1.835 V, while the other is changed from 1.625 to 1.875 V. A difference of 0.03 V can be tolerated with the pure linear equalizer. Meanwhile, a difference of greater than 0.05 V is tolerated if it is considered as fighting nonlinearity.

The following two figures depict the BER versus the signal drive voltages (peak-to-peak voltage, VPP) of one slide in the range of 0.31 to 0.4 V, while the other is fixed at 0.35 V. These two figures show that it permits an interval of 0.06 V without resisting the nonlinearity. However, an allowable interval is beyond 0.09 V with the hybrid post-equalizer. We also find that the BER performance is the best with the same voltage.

Subsequently, we investigate the performance of the proposed channel estimation algorithm, which is shown in Fig. 4.

For the sake of clarity, the received constellations of different equalizers are: (1) without any post-equalizer;

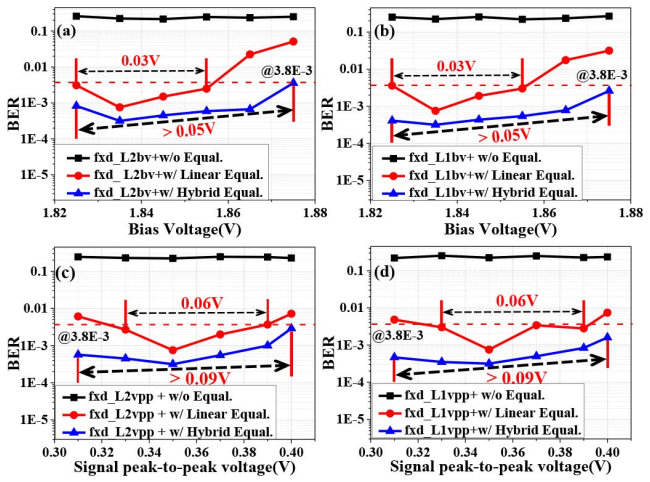

Fig. 3. (a) BER versus DC voltages of LED1; (b) BER versus DC voltages of LED2; (c) BER versus VPP voltages of LED1; (d) BER versus VPP voltages of LED2.

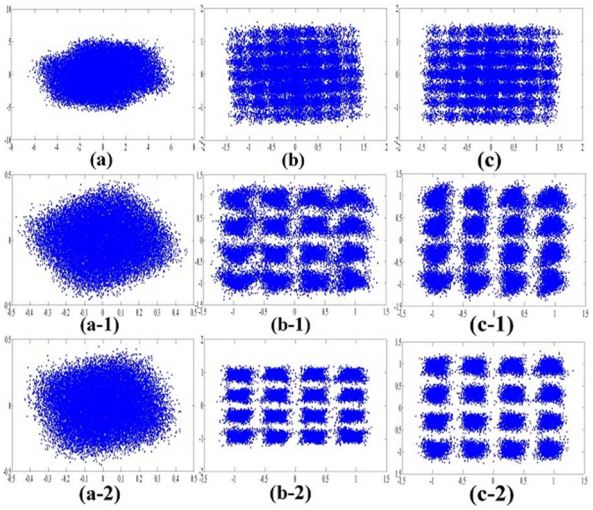

Fig. 4. (a)–(c) 49 constellations before STBC decoding of (1), (2), and (3); (a-1)–(c-1) 16 constellations after STBC decoding without channel optimization of (1), (2), and (3); (a-2)–(c-2) 16 constellations after STBC decoding with channel optimization of (1), (2), and (3).

(2) only with MCMMA; (3) with the proposed hybrid post-equalizer. Wherein, the signals before STBC decoding are shown in Figs. 4(a), 4(b), and 4(c). The constellations without the channel optimization algorithm after STBC decoding are displayed from Figs. 4(a-1) to 4(c-1). We have a better sight of constellations with the proposed channel estimation algorithm, as shown in Figs. 4(a-2) to 4(c-2).

From former works, we conclude that the signals cannot be decoded without any equalization. In the following works, we utilize the case of a pure linear equalizer without proposing an optimization algorithm as the object being compared.

The baud rate in different cases is compared in Fig. 5(a), where the BER of the linear post-equalizer without $H_{\mathrm{opt}}^{-1}(t)$ is higher than the threshold. If taking measures to correct the distorted constellations by nonlinearity, "Volterra" may haul back some of them and guarantee the minimum quality of service (Qos). Meanwhile, a better BER performance is achieved with the optimized channel matrix after STBC decoding.

For clear comparison, we bring the concept of the Q factor, which is inversely proportional to the BER. We measure the Q factor versus the baud rate with the

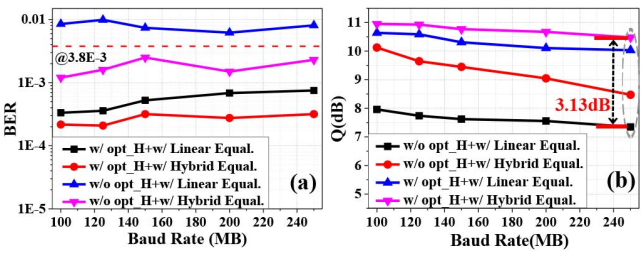

Fig. 5. (a) BER versus baud rate; (b) Q factor versus baud rate.

aforementioned methods. Figure 5(b) shows that with the hybrid post-equalizer and fairly ideal $H_{\text{opt}}^{-1}(t)$, the Q factor is improved by 3.13 dB more than both the case without the nonlinear equalizer and the optimized channel matrix at the baud rate of 250 MB.

Based on the aforementioned works, we draw the following conclusions: the case of combining with the modified hybrid equalizers and proposed channel estimation algorithm uniformly outperform the case of the pure linear equalizer. However, the signals cannot be decoded by the proposed channel matrix with STBC decoding in the case of different signal strengths in both LEDs.

In this Letter, we first present a modified hybrid post-equalizer against both linear distortion and nonlinear distortion. Meanwhile, we design a better channel estimation algorithm to improve the accuracy of STBC decoding. The MISO-STBC model is formulated to verify the correctness of the proposed two algorithms. A transmitting rate of 1.0 Gbit/s over 1.3 m free space is easily achieved. Quantitatively, the Q factor yields a gain of about 3.13 dB with the former two algorithms. The results show the feasibility for future local area network applications.

This work was supported by the National Natural Science Foundation of China (No. 61571133) and the National Key Research and Development Program of China (No. 2017YFB0403603).

References

1. N. Chi, H. Haas, M. Kavehrad, T. D. C. Little, and X. Huang, IEEE Wireless Commun. **22**, 5 (2015).
2. Y. Wang, Y. Wang, N. Chi, J. Yu, and H. Shang, Opt. Express **21**, 1203 (2013).
3. Y. Wang, L. Tao, X. Huang, J. Shi, and N. Chi, IEEE Photon. J. **7**, 1 (2015).
4. Z. Wang, M. Zhang, S. Chen, and N. Chi, Chin. Opt. Lett. **15**, 030602 (2017).
5. N. Chi, J. Zhao, and Z. Wang, Chin. Opt. Lett. **15**, 080601 (2017).
6. IEEE Standard 802.15.7, "IEEE standard for local and metropolitan area networks—Part 15.7: Short-range wireless optical communication using visible light," (2011).
7. H. L. Minh, D. O'Brien, G. Faulkner, L. Zeng, K. Lee, D. Jung, and J. Oh, IEEE Photon. Technol. Lett. **20**, 1243 (2008).
8. S. K. Routray, Potentials IEEE **33**, 28 (2014).
9. K. Lee, H. Park, and J. R. Barry, IEEE Commun. Lett. **15**, 217 (2011).
10. J. Grubor, J. W. Walewski, K. D. Langer, and S. Randel, J. Lightwave Technol. **26**, 3883 (2009).
11. J. Zhu, F. Liang, K. Zhang, and Y. Zhang, IEEE Photon. Technol. Lett. **27**, 1667 (2015).
12. L. Zeng, D. O'Brien, H. L. Minh, G. Faulkner, K. Lee, D. Jung, J. Oh, and E. T. Won, IEEE J. Sel. Areas Commun. **27**, 1654 (2009).
13. L. Qiao, S. Liang, X. Lu, Y. Zhou, Y. Jiang, and N. Chi, Opt. Eng. **56**, 1 (2017).
14. J. Shi, Y. Wang, X. Huang, L. Tao, and N. Chi, Microwave Opt. Technol. Lett. **57**, 2943 (2015).
15. J. Shi, X. Huang, Y. Wang, and L. Tao, in *European Conference on Optical Communication IEEE* (2015), p. 1.
16. T. Foggi, G. Colavolpe, and G. Prati, IEEE Photon. Technol. Lett. **18**, 1984 (2006).
17. C. Gong and Z. Xu, IEEE Trans. Wireless Commun. **14**, 5326 (2015).
18. Y. Wang, L. Tao, Y. Wang, and N. Chi, IEEE Commun. Lett. **18**, 1719 (2014).
19. K. Jin, K. Hyun, and K. P. Sang. Electron. Lett. **50**, 1457 (2014).
20. H. Qian, S. J. Yao, S. Z. Cai, and T. Zhou, IEEE Photon. J. **6**, 1 (2014).
21. G. Stepniak, J. Siuzdak, and P. Zwierko, IEEE Photon. Technol. Lett. **25**, 1597 (2013).
22. Y. Wang, L. Tao, X. Huang, J. Shi, and N. Chi, IEEE Photon. J. **7**, 1 (2015).
23. L. Qiao, X. Lu, S. Liang, and N. Chi, in *Optical Fiber Communication (OFC)* (2018), paper Th2A.64.
24. J. Yang, J. J. Werner, and G. A. Dumont, IEEE J. Sel. Areas Commun. **20** 997 (2002).
25. L. Tao, H. Tan, C. Fang, and N. Chi, in *IEEE Progress in Electromagnetic Research Symposium* (2016), p. 4863.
26. Y. Wang and N. Chi, Chin. Opt. Lett. **12**, S23201 (2014).